Petroleum Science 19 (2022) 2879–2894

Contents lists available at ScienceDirect

Petroleum Science

journal homepage: www.keaipublishing.com/en/journals/petroleum-science

Original Paper

Well production optimization using streamline features-based objective function and Bayesian adaptive direct search algorithm

Qi-Hong Feng [a, b], Shan-Shan Li [a], Xian-Min Zhang [a, *], Xiao-Fei Gao [c], Ji-Hui Ni [c]

[a] School of Petroleum Engineering, China University of Petroleum (East China), Qingdao, 266580, Shandong, China
[b] Shandong Institute of Petroleum and Chemical Technology, Dongying, 257061, Shandong, China
[c] CNOOC China Limited, Shenzhen Branch, Shenzhen, 518000, Guangdong, China

ARTICLE INFO

Article history:
Received 28 February 2022
Received in revised form
17 June 2022
Accepted 21 June 2022
Available online 24 June 2022

Edited by Yan-Hua Sun

Keywords:
Well production
Optimization efficiency
Streamline simulation
Streamline feature
Objective function
Bayesian adaptive direct search algorithm

ABSTRACT

Well production optimization is a complex and time-consuming task in the oilfield development. The combination of reservoir numerical simulator with optimization algorithms is usually used to optimize well production. This method spends most of computing time in objective function evaluation by reservoir numerical simulator which limits its optimization efficiency. To improve optimization efficiency, a well production optimization method using streamline features-based objective function and Bayesian adaptive direct search optimization (BADS) algorithm is established. This new objective function, which represents the water flooding potential, is extracted from streamline features. It only needs to call the streamline simulator to run one time step, instead of calling the simulator to calculate the target value at the end of development, which greatly reduces the running time of the simulator. Then the well production optimization model is established and solved by the BADS algorithm. The feasibility of the new objective function and the efficiency of this optimization method are verified by three examples. Results demonstrate that the new objective function is positively correlated with the cumulative oil production. And the BADS algorithm is superior to other common algorithms in convergence speed, solution stability and optimization accuracy. Besides, this method can significantly accelerate the speed of well production optimization process compared with the objective function calculated by other conventional methods. It can provide a more effective basis for determining the optimal well production for actual oilfield development.

1. Introduction

Well production optimization is indispensable in oil field development since proper reservoir production will contribute to high sweep efficiency and oil recovery factor (Tavallali et al., 2013; Wang, 2016; Chen et al., 2017).

At present, the selection method and optimization method are the main methods to design well production. The selection method is to design a limited number of injection-production system schemes artificially based on the experience of reservoir engineers. Through the comparison of the development effects of multiple schemes, the scheme with the best effect is determined. The method is simple and easy to implement, but it is difficult to obtain the optimal scheme (Wang, 2016). With the development of intelligent optimization, the combination of reservoir numerical simulators with optimization algorithms has increasingly become a research direction (Tavallali et al., 2013; Isebor et al., 2014; Oliveira and Reynolds, 2014; Wang, 2016; Zhang et al., 2020). The method makes full use of the optimization algorithm principle to continuously update the well production and eliminate the artificial factors. The optimization objective function generally selects the development effect indicators such as cumulative oil production (COP), economic net present value (NPV), and oil recovery (Fonseca et al., 2015; Wang et al. 2016, 2019). This method has the advantage of automatic optimization solution. However, it needs to call the reservoir simulators to run hundreds of times. Besides, the size of the optimization problem and the internal control of the algorithm also determines the number of iterations (Wang et al., 2015). Yeten believes that in one optimization solution, the running time of reservoir numerical simulator accounts for 99% of the total

* Corresponding author.
E-mail address: spemin@126.com (X.-M. Zhang).

https://doi.org/10.1016/j.petsci.2022.06.016

optimization time (Yeten, 2003). Due to the complex nonlinear relationship between injection-production system and development effect, reservoir heterogeneity, fluid properties, and other factors affect the optimal well production (Feng et al. 2013, 2014; Wang et al., 2016), so the well production optimization problem is a complex mathematical problem (Bellout et al., 2012; Wang et al., 2019). In addition, the uncertainty in the optimization process might become more time-consuming (Arouri and Sayyafzadeh, 2020; Mahjour et al., 2022). Therefore, two approaches are commonly used to speed up the optimization process and shorten the solution time. One of the approaches is to improve the optimization algorithm efficiency. Meanwhile, the evaluation of the objective function can be sped up to solve the problem.

Reservoir engineering methods, streamline-based simulation, and proxy model are usually applied to reduce the objective function evaluation time. Reservoir engineering methods mainly include injection-production splitting method and equivalent seepage resistance method (El-Khatib, 1997; Feng et al., 2013; Wang, 2016; Mollaei and Delshad, 2019). These methods can quickly predict the reservoir development index, but the specific calculation process is complicated, and the derivation for complex reservoirs is difficult, so the application scope is limited. The streamline simulation method (Al-Najem et al., 2012) is solved by the implicit pressure explicit saturation (IMPES) method (Osako et al., 2009; Gladkov et al., 2013). The computing time is shorter than traditional numerical simulators (Siavashi et al., 2016). Therefore, the streamline-based simulator can be used to speed up the optimization process when calculating the objective function. Thiele and Batycky used streamline simulation to optimize the allocation scheme of injection-production fluid and realized the flow field and well pattern matching (Thiele and Batycky, 2003). Liu established the method of effect evaluation and formed the injection-production optimization method by using differential evolution (DE) algorithm (Liu, 2018). The proxy model method is also a common method to improve the optimization efficiency (Caers, 2003; He et al., 2016; Wang et al., 2022). This method trains the reservoir production index data set through a certain number of numerical simulations sampling, and then constructs a surrogate prediction model similar to the original numerical simulations (Zhang et al., 2020). The proxy model can be used to predict the development effect index, which greatly reduces the operation times of calling the reservoir numerical simulator (Zhou et al., 2007; Onwunalu et al., 2008; Knudsen and Foss, 2015). Many scholars (Wang et al., 2019; Wu et al., 2020; Zhang et al., 2020) used the artificial neural network to construct a proxy model and toke the cumulative oil production or NPV as the objective function. The high computational costs of well production optimization process and reservoir simulations hinder the optimization efficiency despite the fact that these methods can reduce the number of reservoir simulations and speed up the well production optimization process to some extent.

Another way to improve the well production optimization efficiency is to apply or construct an efficient optimization algorithm. The algorithm can be divided into derivate algorithm and derivate-free algorithm according to whether the gradient information is needed. The efficiency of finite-difference method (Sarma et al., 2005; Li et al., 2013) is greatly affected by the number of reservoir model grids. The adjoint gradient method has high efficiency in solving this problem, but needs nested reservoir numerical simulator to obtain the derivatives (Yan et al., 2013), which makes the solution process more complicated. However, the derivate-free optimization algorithm does not need to provide the gradient information of the objective function, and can be directly solved according to the optimization mechanism within the algorithm. The common derivate-free optimization algorithms include DE (Awotunde, 2014), genetic algorithm (GA) (Ambia, 2012), particle swarm optimization (PSO) algorithm (Perez and Behdinan, 2007) and simulated annealing (SA) algorithm (Beckner and Song, 1995). Isebor et al. combined PSO and pattern search to optimize well placement and well production (Isebor et al., 2014). Jinn-Tsong Tsai et al. proposed that dominant individuals generate a new mutation strategy according to the trend of orthogonal vectors, which increases the search ability of the DE algorithm (Tsai, 2015). In addition, some new and efficient optimization algorithms, such as artificial bee colony (ABC) algorithm (Zhang, 2018), covariance matrix adaptation evolution strategy (CMA-ES) (Wang et al., 2019), simultaneous perturbation stochastic approximation (SPSA) (Pouladi et al., 2020; Salehian et al., 2021), are also applied to solve well production optimization problems. Compared with derivate algorithms, this type of algorithm has a simple optimization process. But the derivate-free algorithm is easy to cause the optimization process to fall into a local optimum. On the efficiency of solving all optimization problems, only one basic algorithm cannot be implemented (AlQahtani et al., 2012; Nwankwor et al., 2013; Isebor et al., 2014; Semnani et al., 2022). Therefore, researchers usually couple the optimization mechanisms of two or more optimization algorithms to improve the well production optimization efficiency. One way is to combine derivate algorithm (such as conjugate gradient) (Sampaio et al., 2015) with derivative-free algorithm, which has good performance in finding global and local optimal solutions. In order to improve the ability of generating the optimal solutions, another method combines two derivative-free algorithms and can effectively maintain the diversity of population (Nwankwor et al., 2013; Nasir et al., 2020). Bayesian adaptive direct search optimization (BADS) is a recently developed global-local random search algorithm (Gramacy and Le Digabel, 2015; Acerbi and Ma, 2017). BADS has the advantages of fast convergence, high flexibility and good consistency. However, to the best of our knowledge, the BADS algorithm has not been used to deal with well production problems. Therefore, BADS is applied to well production optimization in this paper.

For large-scale reservoirs, the running time of a single numerical simulation can take minutes to hours or even days, which cannot meet the requirements of field applications. Therefore, in order to improve the well production optimization efficiency, we propose a well production optimization method using streamline feature-based objective function and BADS algorithm. This new objective function, which represents the water flooding potential, is extracted from streamline features. The objective function only needs to call the streamline simulator to run one time step, instead of calling the simulator to calculate the target value at the end of development, which greatly reduces the running time of the simulator. Then the well production optimization model is established and solved by BADS algorithm. The feasibility of the new objective function and the efficiency of the optimization method are verified by three examples. Example I validates the feasibility of the new objective function through the relationship between the new objective function and the cumulative oil production. The convergence speed and search accuracy of BADS and other four algorithms are compared and analyzed in example II. In example III, two conventional optimization methods and the method established in this paper are applied to optimize well production in the egg model.

This paper is organized as follows. In Section 2, the streamline feature-based objective function for well production optimization problem is presented. In Section 3, the BADS optimization algorithm is introduced. In Section 4, the feasibility of the new objective function and the efficiency of the optimization method are verified by three examples. In Section 5, conclusions of this research and prospects for future work are discussed.

2. Streamline feature-based objective function

2.1. Instantaneous flow field potential coefficient (IFPC)

The flow field distribution is directly related to the development effect. The adjustment of well production will result in the redistribution of flow field, which affects the development performance. Therefore, by extracting streamline attribute information, an index representing water flooding ability along streamlines can be constructed to quantitatively reflect the development effect.

Therefore, the instantaneous flow field potential coefficient (IFPC) considering streamline characteristics is established. IFPC has two advantages. The IFPC index comprehensively considers the influence of movable oil saturation and fluid velocity along streamlines. That is, the larger the index, the greater the influence of flow field on the whole movable oil region, indicating that the better the water flooding effect in the future. Besides, it is only necessary to call the streamline simulator to simulate the instantaneous development of the adjusted field, and not necessary to simulate each iteration until the end of development to calculate the objective function, which can significantly reduce the optimization time. In Section 2.2 and 2.3, we construct the IFPC and establish the streamline feature-based objective function for well production optimization problem. And we justify the superiority and feasibility of the new objective function in Section 4.1.

2.2. Construction of IFPC

2.2.1. Principle of streamline numerical simulation

Streamline numerical simulation technology is the process of converting a 3-D model into a 1-D streamline model. The basic principle is as follows. First, the simulator is performed grid division and assign initial values, such as porosity, permeability, saturation, pressure, phase permeability, and well information. Based on this, the IMPES method (Siavashi et al., 2012; Ahmadpour et al., 2016) is used to calculate the pressure field and velocity fields. Then, the streamline field is generated by using Pollock streamline tracing (Pollock, 1988), and the parameter, namely saturation, is obtained along the streamline. Use the obtained saturation distribution along the streamlines to map back to the base grid system. Thereby, the saturation distribution on the grid is calculated.

Since the fluid flow in the streamline simulation is one-dimensional migration along the streamline according to the direction of the pressure gradient (Al-Najem et al., 2012), rather than three-dimensional movement on the grid. Therefore, in order to accurately and truly reflect the fluid flow, the method of using streamlines is closer and more accurate than the method of determining the fluid distribution based on grids. And the flow distribution along the streamline is to fix the volume flow on each streamline, so that the number of streamlines changes with the flow rate of the injection well (Lv, 2009). Therefore, when the injection volume of the injector is larger, the number of streamlines generated on the grid of the well is higher. When a producer produces a larger volume of fluid, more streamlines flow into the well. And the area with higher streamline density, the higher the fluid velocity and vice versa.

Therefore, the streamline simulation can more intuitively and accurately characterize the main fluid flow regions. To further improve the water flooding effect, it is necessary to readjust the flow field in the ultra-high water cut stage. Through the flow field adjustment, the ineffective migration of reservoir fluid is changed into orderly flow, and the flow field is redistributed (Ghori et al., 2006).

2.2.2. Extraction of streamline characteristic parameters

After running the streamline simulation, the obtained streamline data are stored in the formatted files. Take Schlumberger's Frontsim simulator as an example. The Frontsim simulator currently adopted a time-step streamline field corresponding to a streamline file (Schlumberger, 2015). The streamline file format consists of one SLNxxxx file for every report step and one SLNSPEC file. The generated streamline files mainly preserve the geometry and properties of streamlines, including the spatial position coordinates of the streamlines, the flow velocity and saturation distribution of oil and water phases on the streamlines. To control the file size, string information is stored in ASCII encoding, and UNIX-Fortran unformatted binary files are used to store streamline attribute information. Decoding streamline files at each time step (Li et al., 2022), we can obtain the relevant streamline properties:

a) **Streamline position attribute:** For the three-dimensional streamline field, the position attribute of a streamline is characterized by a starting position point, a terminating position point, and multiple intermediate points. The attribute reflects the region and position of the streamline, while these points join together to constitute a complete streamline. Therefore, the streamline field can be restored according to the streamline position attributes. As seen in Fig. 1 for report step 1, assume a water-oil case with three streamlines. Three streamlines start at the injector "INJ1" and terminate in producer "PROD1". Using the decoded streamline data, we can obtain the relevant streamlines in Fig. 1.
b) **Water saturation:** It represents the average water saturation between two nodes on the streamline, which can be used to calculate the remaining oil saturation and characterize the remaining oil recovery potential of the area flowed along the streamline.
c) **Fluid velocity**: It represents the velocities of water and oil flowing along the streamline, and is the embodiment of the fluid flow capacity on the streamline.
d) **Grid ID:** It describes the grid flowed along the streamline. The starting point number on the streamline are the initial injection wells and the final production wells specified by the streamline. It can be used to determine the streamline attribution of the injection-production units.

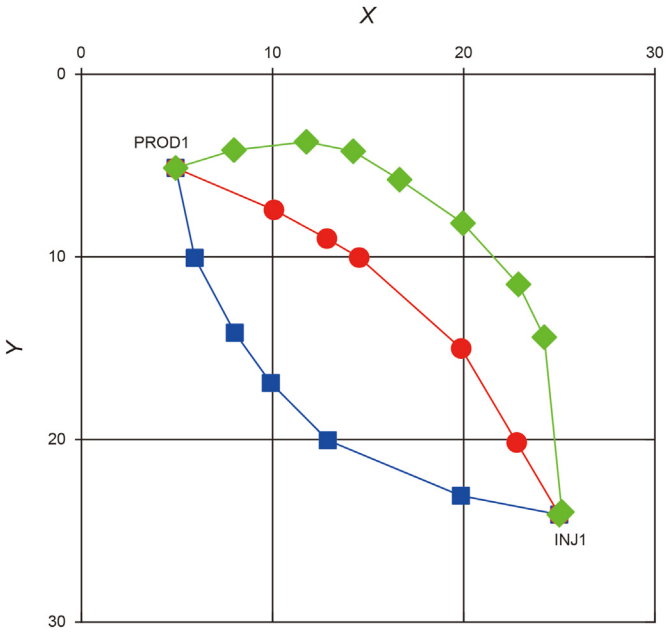

Fig. 1. Streamline computed by Frontsim simulator.

2.2.3. Performance index construction

According to the extracted attribute information of streamlines, the performance index of well production optimization problem is constructed. We choose the fluid velocity and the water saturation on the streamline as basic indicators for the following reasons. The flow field is dynamic, and these indices are mainly selected to describe the dynamic characteristics. Thus static geological parameters such as porosity and permeability are not considered. Secondly, since pressure is an indicator in the flow field displacement process, the greater the pressure difference, the greater the fluid velocity, and there is a causal relationship between them. Therefore, fluid velocity is chosen. In addition, water saturation is the ratio of water phase volume to total fluid volume on the streamline, which can be used to reflect the amount of remaining oil and characterize the development potential of the flow field region. Therefore, it is also selected.

However, due to the numerical dissipation problem (Jimenez et al., 2005) of streamline simulations, the oil and water velocities may approach to zero on some streamlines, wherein the flow capacity at the nodes of streamlines cannot be directly characterized by the oil and water velocities. Meanwhile, the water phase permeability is usually high, and the water saturation increases linearly in the later stage of oilfield development, which cannot obviously characterize the flow field. Therefore, we defined two parameters, that is, the remaining oil displacement efficiency of streamline and the oil-water displacement pressure difference ratio of streamlines to characterize the flow field.

Remaining oil displacement efficiency of streamline refers to the ratio of current movable oil saturation to original movable oil saturation on the streamline, and their formula are as follows. Among them, Eq. (1) is the remaining oil displacement efficiency of the streamline node, and Eq. (2) calculates the average remaining oil displacement efficiency of the streamline.

$$E_{roij}=\frac{1-S_{wij}-S_{or}}{S_{oinit}-S_{or}} \tag{1}$$

$$E_{roi}=\sum_{j=1}^{n_i}E_{roij}/n_i \tag{2}$$

where E_{roij} is the remaining oil displacement efficiency of the streamline node (i, j); S_{wij} is the water saturation of the streamline node (i, j); S_{oinit} is the initial oil saturation; S_{or} is the residual oil saturation; n_i is the total number of nodes of the i-th streamline; E_{roi} is the average remaining oil displacement of the i-th streamline; subscript i is the streamline number; subscript j is the number of streamline nodes.

This index is defined to reflect the movable oil saturation of the streamline and it can be used to characterize the development potential of the flow field area. The larger the index value, the more movable oil is not affected by the injected water along the streamline direction at this moment. That is, the higher the sweeping degree of the streamline to the high movable oil saturation region, the greater the development potential.

Oil-water displacement pressure difference ratio of streamline refers to the pressure displacement difference ratio of oil phase and water phase on the streamline. The formulas are Eqs. (3) and (4).

$$\Delta P_{owij}=\frac{\mu_o\cdot v_{oij}}{K_{ro}(S_{wij})}\Big/\frac{\mu_w\cdot v_{wij}}{K_{rw}(S_{wij})} \tag{3}$$

$$\Delta P_{owi}=\sum_{j=1}^{n_i}\Delta P_{owij}/n_i \tag{4}$$

where ΔP_{owij} is the oil-water displacement pressure difference ratio of the streamline node (i, j); v_{wij} and v_{oij} are the flow rates of water phase and oil phase of the streamline node (i, j); μ_w and μ_o are the viscosity of water phase and oil phase, respectively, mPa s; $K_{ro}(S_{wij})$ and $K_{rw}(S_{wij})$ are the relative permeability of oil phase and water phase corresponding to the water saturation of the streamline node (i, j), respectively; ΔP_{owi} is the average oil-water displacement pressure difference ratio of the i-th streamline.

Wherein, the relative permeability of oil phase and water phase corresponding to the water saturation is calculated by the following expressions (Goda and Behrenbruch, 2004).

$$K_{ro}(S_{wij})=K_{ro}(S_{wmin})\left[\frac{S_{wmax}-S_{wij}-S_{or}}{S_{wmax}-S_{winit}-S_{or}}\right]^{c_o} \tag{5}$$

$$K_{rw}(S_{wij})=K_{rw}(S_{or})\left[\frac{S_{wij}-S_{wc}}{S_{wmax}-S_{wc}-S_{or}}\right]^{c_w} \tag{6}$$

where S_{wc} is the bound water saturation; S_{winit} is the initial water saturation; S_{wmin} and S_{wmax} are the minimum and maximum water saturation values in the relative permeability curve, respectively; $K_{ro}(S_{wmin})$ is the relative permeability of oil phase at minimum water saturation; $K_{rw}(S_{or})$ is the relative permeability of water phase at residual oil saturation; c_o and c_w are oil and water phase permeability curve index, respectively, which can be obtained by fitting the permeability curve.

This index is constructed to reflect the flow capacity between oil and water in the flow field, which can used to characterize the water flooding capacity in the flow field areas. When the velocity of oil phase is greater than that of water phase on the streamline, it means that the former has stronger flow capacity. Therefore, the larger the value, the stronger the oil flow capacity along the streamline direction, or the stronger the water flooding capacity.

The calculated E_{roi} and ΔP_{owi} on each streamline were arithmetically averaged, respectively. The overall remaining oil displacement efficiency (E_{ro}) and overall oil-water displacement pressure difference ratio (ΔP_{ow}) of the flow field at this moment can be obtained. The calculation expressions are:

$$E_{ro}=\sum_{i=1}^{L}E_{roi}/L \tag{7}$$

$$\Delta P_{ow}=\sum_{i=1}^{L}\Delta P_{owi}/L \tag{8}$$

where E_{ro} is the overall remaining oil displacement efficiency of the flow field at a certain time; ΔP_{ow} is the overall oil-water displacement pressure difference ratio of the flow field at a certain time; L is the total number of streamlines in the flow field at a certain time.

E_{ro} can reflect the overall change of the remaining oil displacement efficiency in the flow field corresponding to different development moments. The larger the value, the more movable oil area the streamline flows through at this moment. That is, the oil displacement efficiency of the streamline to the movable residual oil is higher. Besides, ΔP_{ow} can reflect the difference in oil-water flow capacity of the flow field corresponding to different development times. If the displacement pressure difference of the oil phase on the streamline is higher than that of the water phase, it means that the flow capacity of the oil phase is higher than that of the

water phase, and the resistance of water displacement oil is relatively small.

In order to comprehensively reflect the development effect of the reservoir, a comprehensive index to characterize the flow field is constructed based on E_{ro} and ΔP_{ow}. That is, the flow field potential coefficient, which is called by "C_{fp}", and the calculation formula:

$$C_{fp} = E_{ro} \times \Delta P_{ow} \tag{9}$$

where C_{fp} is the flow field potential coefficient.

The flow field potential coefficient can comprehensively characterize the matching relationship between movable oil saturation and oil-water driving capacity in the flow direction of each streamline. The larger the coefficient, the greater the overall influence of the flow field on the movable oil region, and the stronger the oil phase movable capacity. The greater the corresponding water flooding development potential, the better the future water flooding effect. If the water flooding effect becomes better, it means that more streamlines in the flow field control the highly saturated oil region and improve the remaining oil production capacity. Therefore, this coefficient can be used to quantitatively reflect the water flooding effect of reservoir flow field adjustment.

The variation of streamline distribution is synchronized with the adjustment measures taken by the reservoir. When the flow field adjustment measures are completed, the underground streamline will also be redistributed. The flow field potential coefficient at this time represents the maximum water flooding potential. Therefore, the flow field potential coefficient calculated instantaneously after the completion of flow field adjustment is defined as the "instantaneous flow field potential coefficient", referred to as "IFPC".

2.3. Streamline features-based objective function

Therefore, the maximum "IFPC" is used as the objective function of well production optimization problem.

$$\begin{aligned}
&\max\ \mathrm{IFPC} = \sum_{i=1}^{L}(E_{roi}(\mathbf{Q}))\times\sum_{i=1}^{L}(\Delta P_{owi}(\mathbf{Q}))/L^2\\
&s.t.\quad q_{m\min}^{inj} \le q_m^{inj} \le q_{m\max}^{inj},\quad m=1,2,\cdots,r\\
&\qquad q_{n\min}^{pro} \le q_n^{pro} \le q_{n\max}^{pro},\quad n=1,2,\cdots,s\\
&\qquad \sum_{m=1}^{r} q_m^{inj} = Q_{inj}\\
&\qquad \sum_{n=1}^{s} q_n^{inj} = Q_{pro}\\
&\qquad Q_{inj} = Q_{pro}
\end{aligned} \tag{10}$$

where $\mathbf{Q}$ is the fluid rate, m^3/d; Q_{inj}, Q_{pro} are the total water injection rate and the total oil production rate, respectively, m^3/d; q_{min}^{inj}, q_{max}^{inj} are the minimum and maximum water injection rate, respectively, m^3/d; q_{min}^{pro}, q_{max}^{pro} are the minimum and maximum oil production rate, respectively, m^3/d; subscripts r, s are the number of injection wells and production wells, respectively.

The objective function can reflect the matching degree of movable oil saturation distribution and oil-water driving ability in each flow direction. This objective can evaluate the long-term development effect of the flow field adjustment. The higher the objective value, the higher the corresponding final cumulative oil production, and the better the water flooding effect. When solving the injection-production optimization problem, each iteration only needs to call the streamline simulator to run one time step and calculate the target. The objective function greatly reduces the running times and improves the optimization efficiency.

3. Bayesian adaptive direct search optimization algorithm

BADS, proposed by Acerbi and Ma (2017), is a global-local random search algorithm. BADS is a hybrid Bayesian optimization (BO) (Jones et al., 1998) method that combines the mesh adaptive direct search (MADS) (Audet and Dennis, 2006) framework with a BO search performed by a local Gaussian process (GP) surrogate, and implements it through some heuristics to improve the efficiency.

BADS alternates between a series of fast local BO steps (the search stage of MADS) and a systematic, slower exploration of the mesh grid (poll stage) (see Fig. 2). These two stages complement each other, and in the search stage we can efficiently explore the space and provide an adequate surrogate model. When the search stage fails repeatedly, which means that the GP model cannot help optimization (e.g., due to the specified error model, or excess uncertainty), BADS switches to the poll stage. Fail-safe and model-free optimization is performed in poll stage, in which BADS collects information about the local shape of the objective function to construct a better proxy for the next search stage. In this algorithm, sampling points generated in the process of BO are used as the assistant method of MADS algorithm to search for advantages, which improves the success rate of sample points selection and reduces the number of iterations of the algorithm. Therefore, BADS algorithm can improve the optimization efficiency and convergence speed.

3.1. Search stage

In the search stage, a Gaussian process is fit to a local subset of the points evaluated so far. Then, we iteratively choose points to evaluate according to a lower confidence bound strategy that trades off between exploration of uncertain regions (high GP uncertainty) and exploitation of promising solutions (low GP mean). The process is calculated by the mesh size parameter Δ_k^m and the mesh direction set D, among which the mesh size parameter Δ_k^m is used to control the search range.

Before the kth iteration, the optimal solution of the objective function is denoted as x_k, and the set of calculated feasible solutions is defined as S_k. The set formed by all search points is defined as M_k, and its expression is as follows:

$$M_k = \{x \in S_k\} \cup \{x_k + \Delta_k^m D\mathbf{z}\} \tag{11}$$

where $\mathbf{z}$ is a full rank positive integer matrix, $\mathbf{z} \in Z_+^p$; p is the number of direction vectors; Z_+ is a set of non-negative integers.

There are four steps involved in the search stage.

Step 1: Constructing grid cells with x_k as search center.

Step 2: Calculate the target value of finite grid points near the construction grid element and find the feasible solution to improve the objective function.

Step 3: If a feasible solution to improve the objective function is

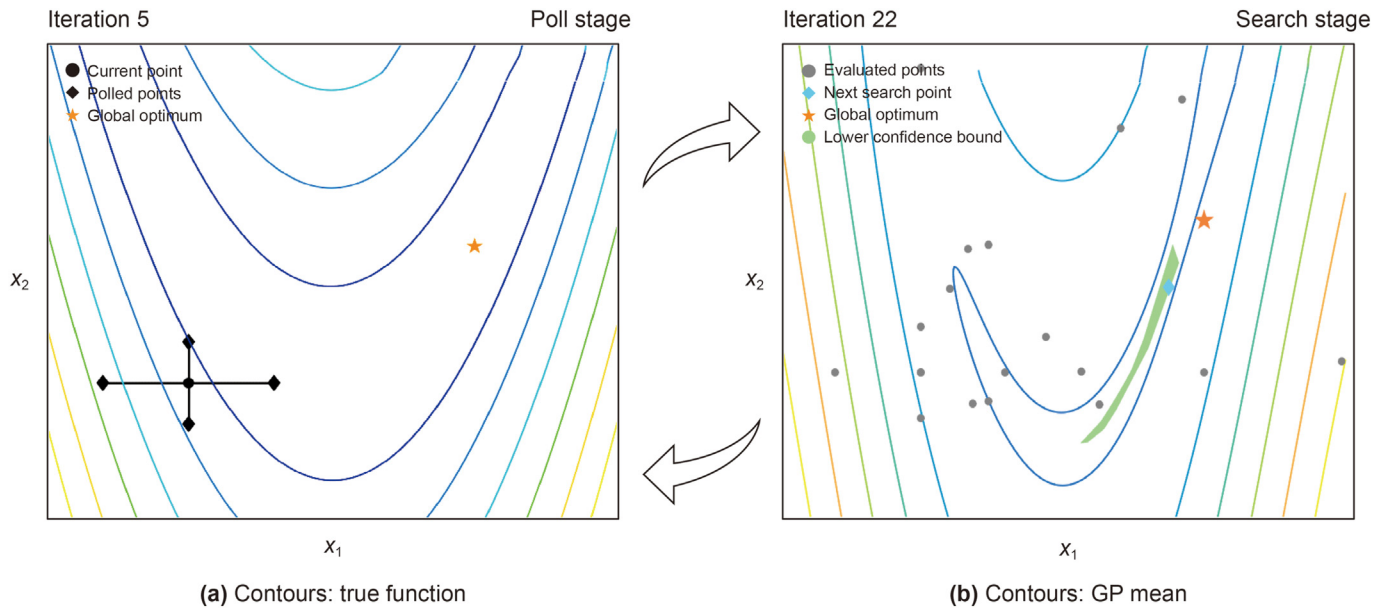

Fig. 2. BADS procedure (Acerbi and Ma, 2017).

found, the search is successful. At this point, move the grid center to the place, and the mesh size parameter Δ_{k+1}^{m} is increased at the $k+1$ iteration step.

Step 4: Failure to find a feasible solution to improve the objective function indicates that the search process of the iteration step fails. Then turn to the next optimization step, that is, the poll stage. At the same time, the grid size parameter Δ_{k+1}^{m} is reduced at the $k+1$ iteration step.

3.2. Poll stage

When the search stage fails to find a feasible solution to improve the objective function, the poll stage is performed. In the poll stage, points are evaluated on a mesh by taking steps in one direction at a time, until an improvement is found or all directions have been tried. The step size is doubled in case of success, halved otherwise. This process is controlled by the size parameter Δ_{k+1}^{p} of the screening frame.

In the poll stage, the set composed of directions with large density in the feasible search range is defined as the screening point set P_k, where $\mathbf{D}_k$ is the matrix composed of column elements in the grid direction set.

$$P_k = \{x_k + \Delta_k^m d : d \in \mathbf{D}_k\} \subset M_k \tag{12}$$

During the whole poll stage, the parameter Δ_k^m should be less than the parameter Δ_{k+1}^{p}. When a feasible solution to improve the objective function is found, it shows that the poll stage of the iterative step is successful. At this moment, move the mesh center to the improvement point and continue the next poll stage. When the objective function is not improved, it indicates that the iterative step is failed. At this time, the control parameters Δ_{k+1}^{p} and Δ_k^m are reduced, and the reduction speed of Δ_{k+1}^{p} is guaranteed to be less than that of Δ_k^m. In the poll stage, it is easy to fall into a limited set, so this update method is adopted to avoid it, to improve the probability of finding the optimal direction.

In this stage, the optimization strategy of global pattern search optimization (GPS) is extended by generating the set of screening points, and the local optimization and direction can be screened. Hence the BADS algorithm has a fast convergence speed and efficient local optimization ability.

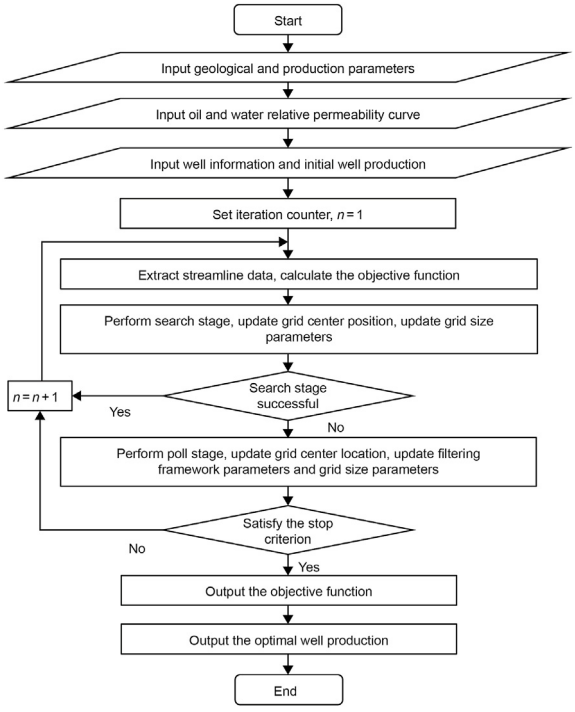

Fig. 3. Flow chart of well production optimization with IFPC-based BADS optimization.

3.3. IFPC-based BADS optimization description

Fig. 3 shows the flow chart of well production optimization using streamline features-based objective function and BADS algorithm. We refer to this method as the IFPC-based BADS optimization in the next section.

4. Results and discussion

In this section, the relationship between the objective function and the cumulative oil production is obtained by giving fluid flow schemes for different producers in the reservoir randomly, and the feasibility of the objective function is verified. Then, the well production in the egg model are optimized using IFPC-based BADS optimization method. And the efficiency and accuracy of BADS algorithm is verified compared with other four common algorithms. Besides, two conventional optimization objective functions and IFPC objective function are used to compare the optimization efficiency, which verifies the efficiency and accuracy of the new method. The Frontsim simulator (GeoQuest, 2016) was used to calculate specific well production data, and the optimization algorithm in MATLAB software (MATLAB, 2019) is used to generate the optimized well production. In the optimization process, the optimal well production can be obtained by coupling Frontsim simulator with MATLAB program.

4.1. Example I: a 2-D heterogeneous model for objective function validation

4.1.1. Reservoir model description

The basic model used in this section is a 2-D heterogeneous reservoir (Christie and Blunt, 2001), which is a cut-off of SPE10 benchmark model. The model is a five-spot well pattern, and model uses 50 × 50 × 1 grid blocks with model size of 360× 360× 20 m^3, and the depth of top phase is 1900 m. Besides, Fig. 4 shows permeability and porosity fields. The oil and water relative permeability curves are plotted in Fig. 5(a). In order to further verify the applicability of the objective function, the oil viscosity and residual oil saturation distribution of the formation are changed. As shown in Table 1, it is the basic parameters of the three reservoir models. The curve in Fig. 5(b) is taken from an actual reservoir.

As shown in Fig. 4, one vertical injector is deployed at the center of the reservoir, and four producers are located in each corner. The injection rate is 80 m^3/d, and the liquid production rate of the four producers is 20 m^3/d, respectively. The reservoir has the same initial water saturation throughout.

To obtain the relationship between the IFPC and cumulative oil production, we developed different fluid distribution schemes for producers. The fluid volume of the injector remains unchanged, that is, 80 m^3/d. And the total liquid production also remains the same, 80 m^3/d. In order to change the liquid production volume of the four producers, we set the value range of the liquid volume of the four producers as 0–80 m^3/d, and the liquid volume is a multiple of 5, that is, 0, 5, …, 80 m^3/d. Therefore, there are 969 liquid distribution schemes for each model. When water cut of the model reaches 95%, the above liquid volume scheme is used for production and developed to the same time. Due to the different distribution of fluid volume in the four producers, corresponding different flow field distributions appear. It makes the calculated instantaneous flow field potential coefficients and the corresponding cumulative oil production also different.

4.1.2. Results and discussion

The Frontsim simulator is used to simulate 969 liquid distribution schemes for each model. The IFPC is calculated by Eq. (9) and the cumulative oil production is calculated by reservoir simulator Eclipse, respectively. The relationship of the IFPC and the cumulative oil production of three reservoir models are shown in Fig. 6. There are a total of 969 points, each of which represents the IFPC and the corresponding final cumulative oil production under a production well fluid distribution scheme. It demonstrates that the IFPC is positively associated with the cumulative oil production. In other words, when the IFPC is higher, the reservoir can achieve a higher cumulative oil production, in which case the streamlines

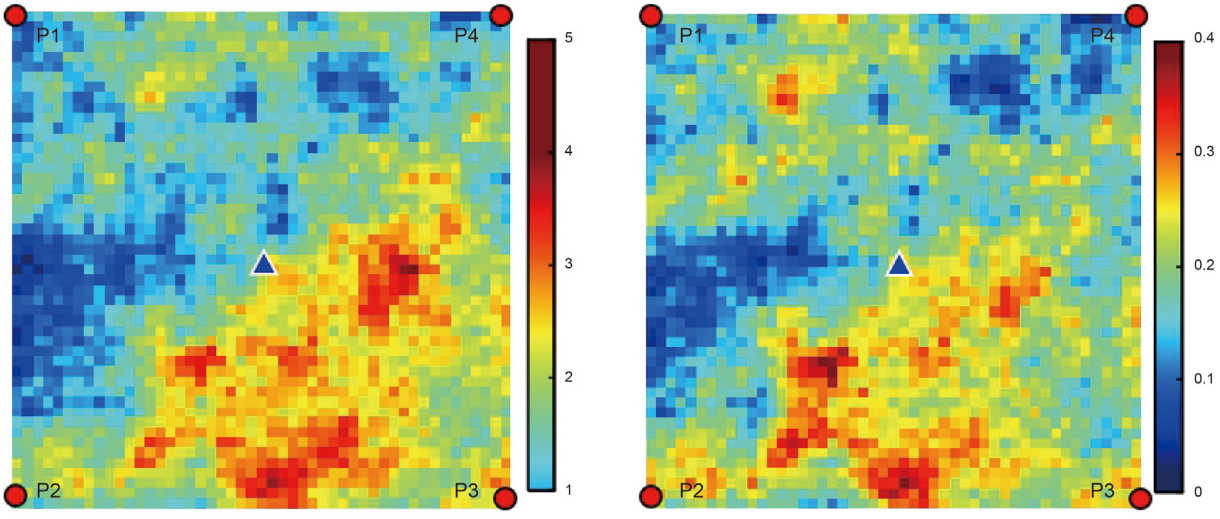

(a) log$k$ **(b)** Porosity ϕ

Fig. 4. Permeability and porosity maps of Example I (k is the permeability).

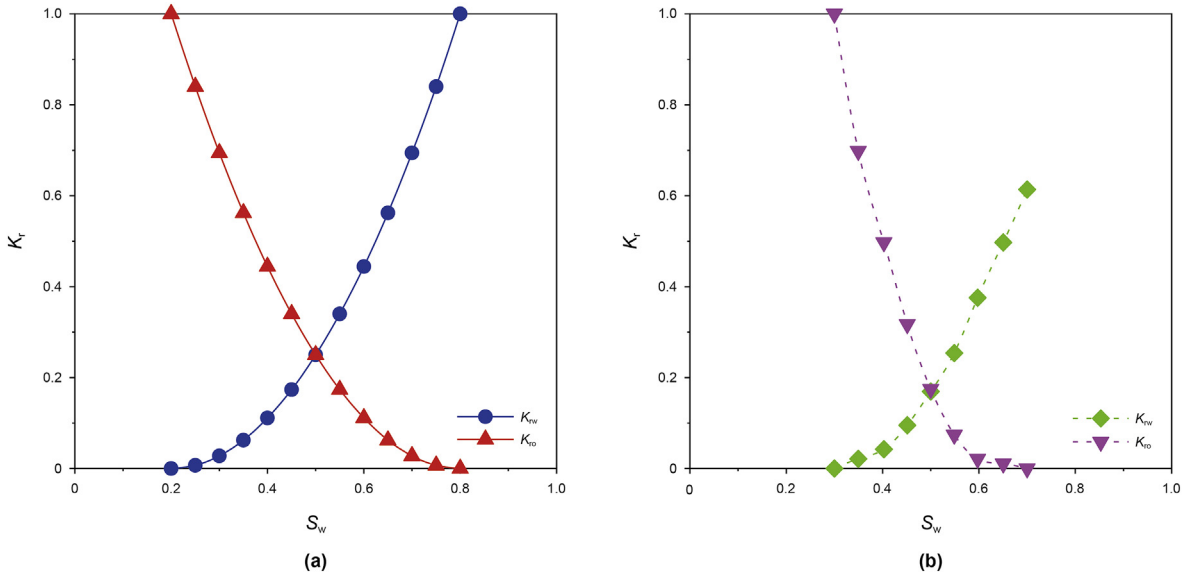

Fig. 5. Oil and water relative permeability curves (S_w is the water saturation; K_r is the relative permeability).

Table 1
Verify the basic parameters of Example I.

Model	Oil and water relative permeability curve	Residual oil saturation	Formation oil viscosity, mPa s
Basic model	Fig. 5(a)	0.2	2.4
Model 1	Fig. 5(a)	0.2	65.0
Model 2	Fig. 5(b)	0.3	30.0

will be concentrated in the high saturation oil region.

As can be seen from Fig. 7 and Table 2, when the IFPC becomes larger, the liquid production rate of the producers P1 and P2 increases under the condition of the same well pattern. It increases the streamline density flowing through the highly saturated remaining oil region. In this case, the more movable oil is displaced from the reservoir in the future, the less oil remains. In the area where the displacement is relatively sufficient, the streamline density is reduced. Therefore, if the liquid volume scheme which can achieve the maximum IFPC is found, the working system corresponding to the maximum cumulative oil production can also be obtained. Thus the feasibility of streamline feature-based objective function in well production problem is proved.

4.2. Example II: egg model for BADS optimization algorithm

4.2.1. Reservoir model description

The egg model is adopted to verify that IFPC-based BADS optimization method can effectively optimize well production. Besides, we selected global pattern search optimization (GSS), multilevel coordinate search optimization (MCS) (Lambot et al., 2002), PSO, CMA-ES, and BADS algorithm respectively to solve the optimization problem. And the optimization performance of these algorithms is compared from the three aspects of the accuracy, convergence speed, and solution stability of the optimization results.

The egg model is represented by $60 \times 60 \times 7 = 25200$ grid cells of which 18,533 cells are active. The grid block size is set to 8 m $\times$ 8 m $\times$ 4 m, and the net to gross thickness ratio is set to 1.0. The details of the geological and fluid parameter settings of the egg model can be found in (Jansen et al., 2015). The longitudinal heterogeneity of the seven layers in the original model is small, so the third layer is selected as the research object. Fig. 8 displays the permeability and the default placement of wells. The model consists of four injectors and eight producers placed, and these wells form a five-spot well pattern. Besides, the model has an average permeability of 1221.10 mD, a porosity of 0.2, and a top depth of 4008 m. We consider an oil-water two-phase flow in this model. The initial rate of individual well in the model is shown in Table 3. The reservoir lifetime is set to 3600 days.

Fig. 9(a) shows the distribution of streamline oil saturation when the water cut of the model is 90%, and the remaining oil saturation distribution at the end of production is presented in Fig. 9(b). The displacement is not balanced in reservoir at present. In order to improve this reservoir development effect, we seek to optimize the liquid rates of four injectors and eight producers with 90% water cut. There are 12 optimization variables. Only bound constraints are considered and the detailed optimization parameters are given in Table 4.

4.2.2. Results and discussion

The complexity of the optimization problem determines the total calculation times of the objection function. Meanwhile, the determination of population number and iterative steps in the optimization algorithm can affect the probability of falling into local optimum. As in previous studies, when the optimization variables are less than 20, the evaluation number of objective functions is usually 1250 to 10000 times (Nwankwor et al., 2013; Jesmani et al., 2016). The egg model has 12 optimization variables in example II. Therefore, when we set the maximum number of iterations to 50 and the population number to 30, the maximum number evaluated by the objective function is 1500. Algorithm parameter setting: (1) For BADS, we use the setting from (Acerbi

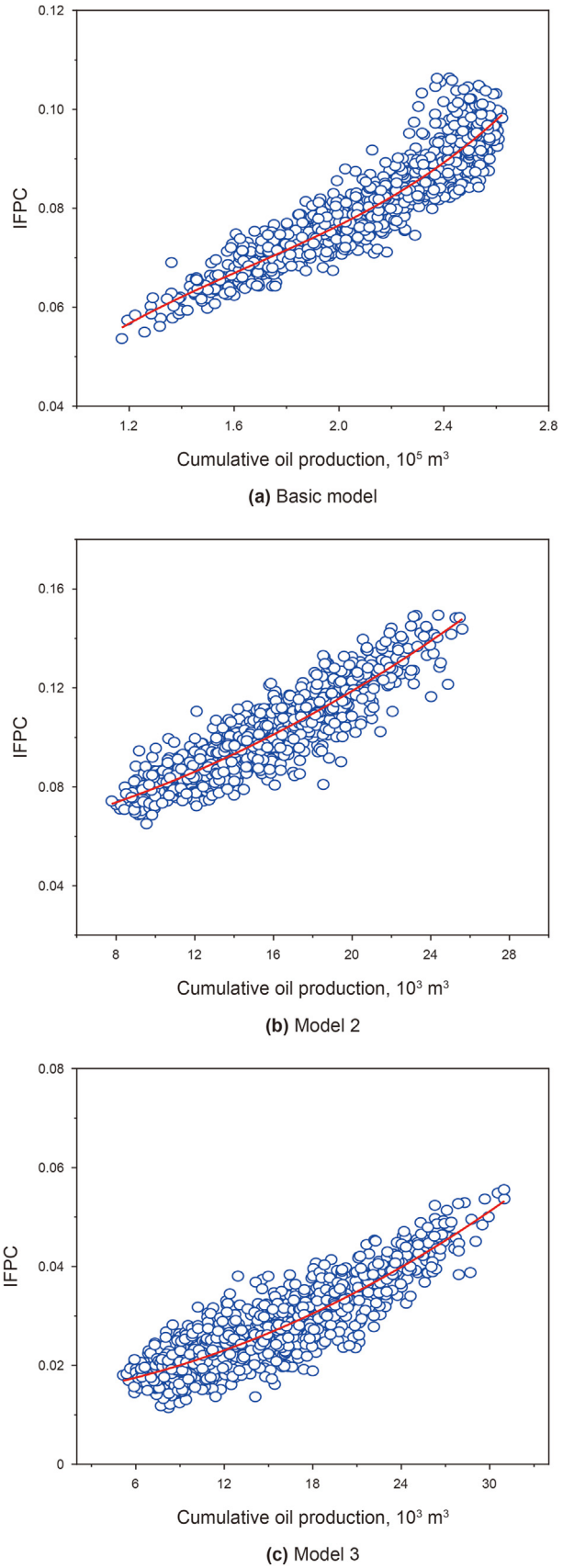

Fig. 6. Cumulative oil production versus IFPC under different liquid distributions.

and Ma, 2017). (2) For GSS parameter settings, we use a $2n$ positive spanning set, where n is the dimension of the search space. The expansion factor is set to 2, and the contraction is set to 0.5. (3) Our implementation of PSO uses the population size of 50, and the weighting parameters $w = 0.9$, $c_1 = 0.5$, and $c_2 = 1.25$. (4) For MCS, the number of levels is chosen as $s_{\max} = 5n + 10$, where n is the dimension of the problem. The maximal number of visits in the local search is 50, and the acceptable relative accuracy for local search is $r = 0.01$. (5) For CMA-ES, we use the setting from (Hansen and Kern, 2004).

Since CMA-ES, PSO, and BADS algorithms belong to the stochastic search algorithm, each optimization result obtained by these algorithms is different. Therefore, to eliminate the influence of randomness on the performance of the algorithm, the same initial point is used for iteration. The average performance obtained by each optimization algorithm running independently for 10 times is considered as the optimal well production. The initial points of the five algorithms adopt the median values of the upper and lower limits of each optimization variable. Thus, the initial solutions corresponding to the initial values of the algorithm are completely the same.

Plots of the IFPC of the five algorithms versus the number of simulation runs are shown in Fig. 10. As in Example II, 10 trials are performed for CMA-ES, PSO, and BADS, and the solid lines depict the average IFPC overall 10 trials. Since GSS and MCS are deterministic algorithms, only one trial is performed.

In terms of convergence speed, there are differences among the five optimization algorithms (Fig. 10). We can see that GSS converges slower than PSO at an early stage, but eventually GSS obtains higher IFPC. Although PSO can search very large space of candidate solutions, and the stochastic element of the movement of the population reduces the chance of getting trapped at an unsatisfactory local optimum, PSO does not guarantee an optimal solution is ever found. Besides, the convergence speed of CMA-ES is higher than that of PSO and GSS. Unlike the population-based stochastic search algorithms, such as GA, PSO, candidate solutions of CMA-ES are sampled from a probability distribution which is updated iteratively. In addition, in the deterministic search algorithm, MCS performs better than GSS in both search speed and search results. However, BADS shows excellent convergence speed at the early stage of optimization (number of function evaluations <200), and IFPC reaches the highest. This is useful for optimization given a limited computational budget. Since BADS algorithm is coupled with MADS and Gaussian process, it can effectively explore space and provide an adequate surrogate model in the search stage. And in the poll stage, the optimization strategy is extended by generating the set of screening points, and the local optimization and direction can be screened. Therefore, BADS has a faster convergence speed and efficient optimization ability compared with other four common algorithms.

Furthermore, we analyzed the randomness of BADS, CMA-ES, and PSO, that is, the stability difference. Fig. 11 shows the range of IFPC for the iterative curves of the three algorithms running 10 times separately, and the shadow section represents the region between the minimum and maximum values in the 10 times optimization process.

In terms of solving stability, BADS has good stability (Fig. 11). In the whole optimization process, PSO has an obvious difference in each operation result and does not converge when the number of iterations reaches 1500. The IFPC has been steadily improving in the whole optimization process, indicating that PSO needs more iterations to find the optimal solution. This is because PSO is a

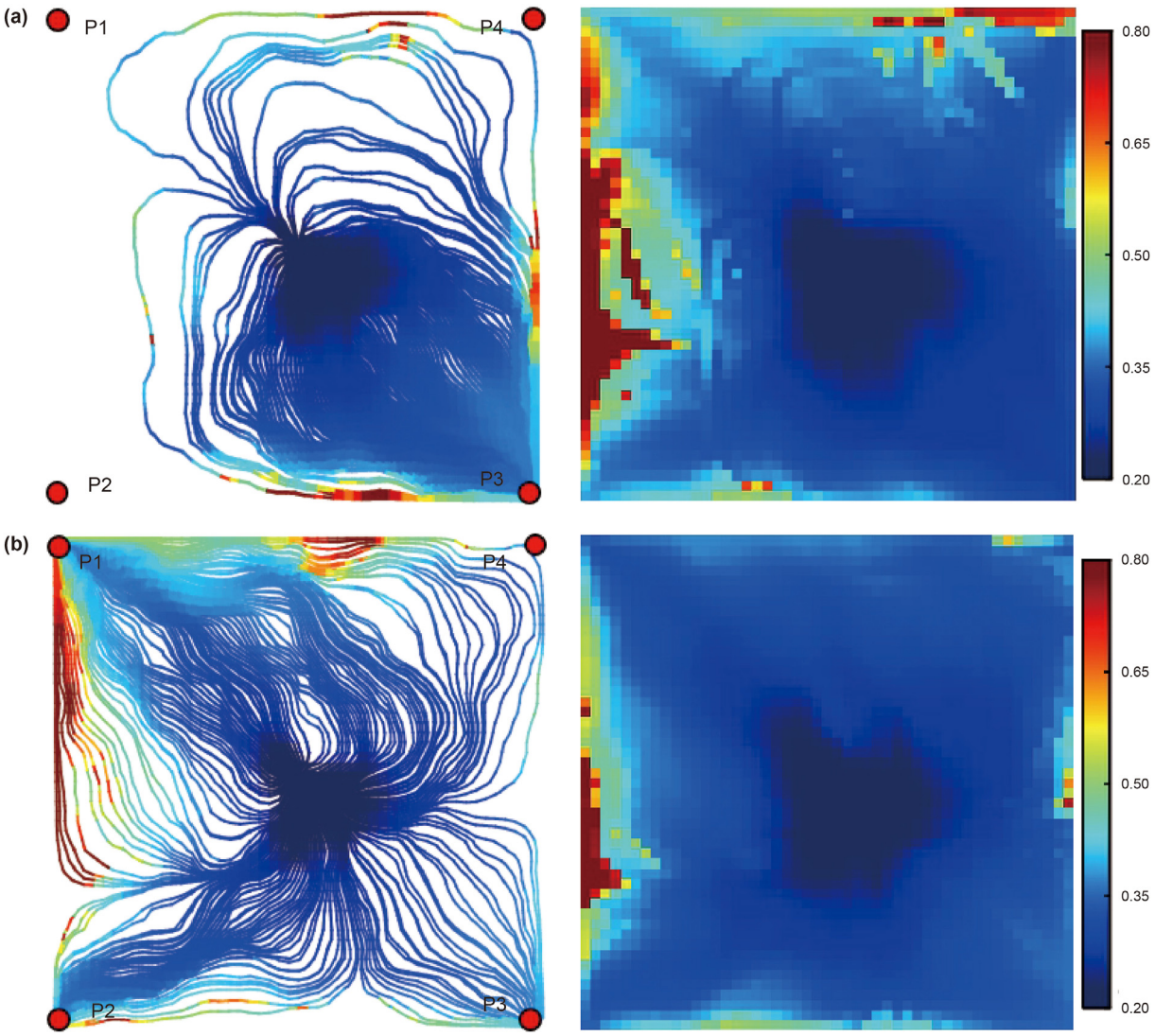

Fig. 7. Instantaneous streamline distribution and residual oil saturation distribution corresponding to the minimum IFPC (**a**) and the maximum IFPC (**b**). Among them, the streamline distribution is the instantaneous distribution after the liquid volume adjustment, and the remaining oil saturation distribution is the distribution after the liquid volume adjustment to the end of development.

Table 2
Fluid production rates of corresponding producers at minimum and maximum IFPCs.

Case	Production rate, m^3/d				Cumulative oil production, 10^5 m^3	IFPC
	P1	P2	P3	P4		
Case 1: Liquid production rate corresponding to the minimum IFPC	0	0	80	0	1.194	0.057
Case 2: Liquid production rate corresponding to the maximum IFPC	50	20	10	0	2.599	0.103

stochastic search algorithm, and its ability to converge to the optimal value is poor. Besides, in the early stage of iterative optimization, the results of 10 times CMA-ES have large fluctuations. And with the increase in iteration steps, CMA-ES convergence difference becomes smaller. This is because CMA-ES is a local search algorithm, which is easy to fall into local optima. In addition, we can see that PSO has converged to different locations for each trial. Compared with CMAES, PSO is more easily falls into local optima in our test cases, in spite of the larger population size and the ability search the entire space. However, BADS is a local-global search algorithm. In the whole optimization process, the difference between each running result is small, and the later optimization can converge to the same value.

To further compare the difference in the optimization accuracy of the algorithms, Fig. 12 presents boxplots of the final IFPC for 10 runs. And the IFPC values of five optimization algorithms are given in Table 5 and Table 6.

According to the boxplot in Fig. 12 and Tables 5 and 6, the BADS algorithm obtains the highest IFPC after 1500 simulation runs. The standard deviation of the BADS algorithm (0.0005) is lower than that of the CMA-ES algorithm (0.0027). The average IFPC of the BADS algorithm (0.3374) is higher than that of the CMA-ES

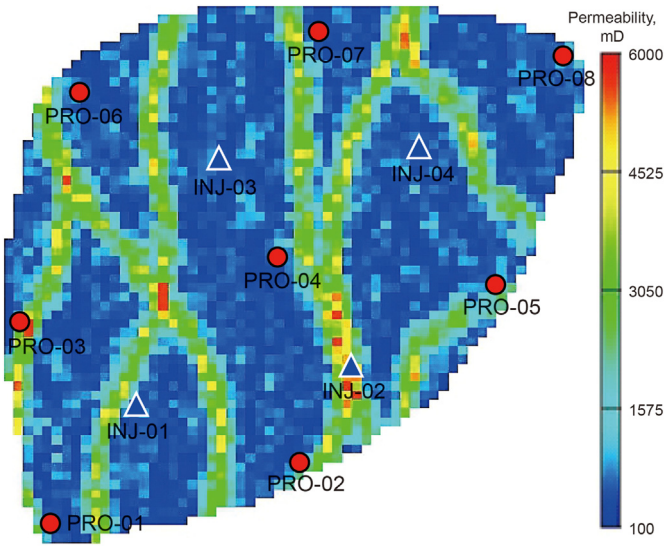

Fig. 8. Egg model displaying the permeability and the well placement for Example II.

Table 3
Initial rate of individual well in Example II.

Well	Initial rate, m^3/d
INJ-01, INJ-04	20
INJ-02, INJ-03	60
PRO-01, PRO-03, PRO-06, PRO-07	10
PRO-04	20
PRO-02, PRO-08	30
PRO-05	40

Table 4
Optimization parameters used in Example II.

Parameter	Value
Optimization variables	12
Minimum rate of injectors, m^3/d	0
Maximum rate of injectors, m^3/d	90
Minimum rate of producers, m^3/d	0
Maximum rate of producers, m^3/d	40

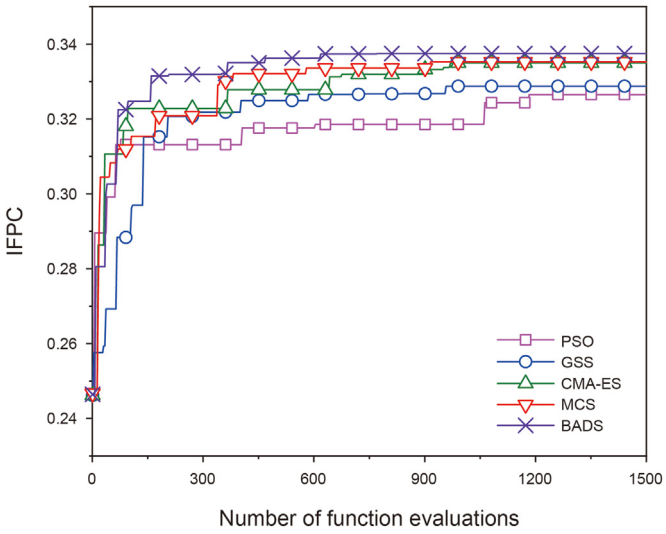

Fig. 10. Optimization performance for Example II.

algorithm (0.3345), increasing by 0.87%. Compared with PSO algorithm, BADS algorithm improves by 3.43%. The standard deviation for the PSO algorithm is larger than the standard deviation for CMA-ES algorithm. Therefore, according to the average IFPC and the standard deviation, the search performance of the BADS algorithm is better than other optimization algorithms.

Based on the above analysis, it can be concluded that the BADS algorithm is superior to other optimization algorithms in convergence speed, solution stability and optimization accuracy.

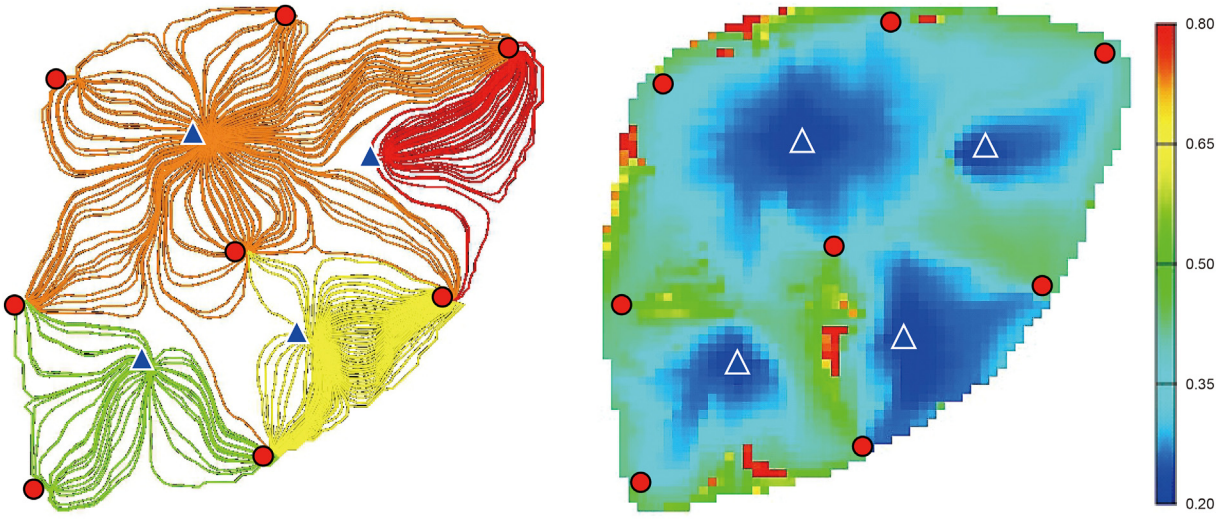

(a) Instantaneous streamline distribution **(b)** Remaining oil saturation distribution

Fig. 9. Streamline and saturation distribution in Example II.

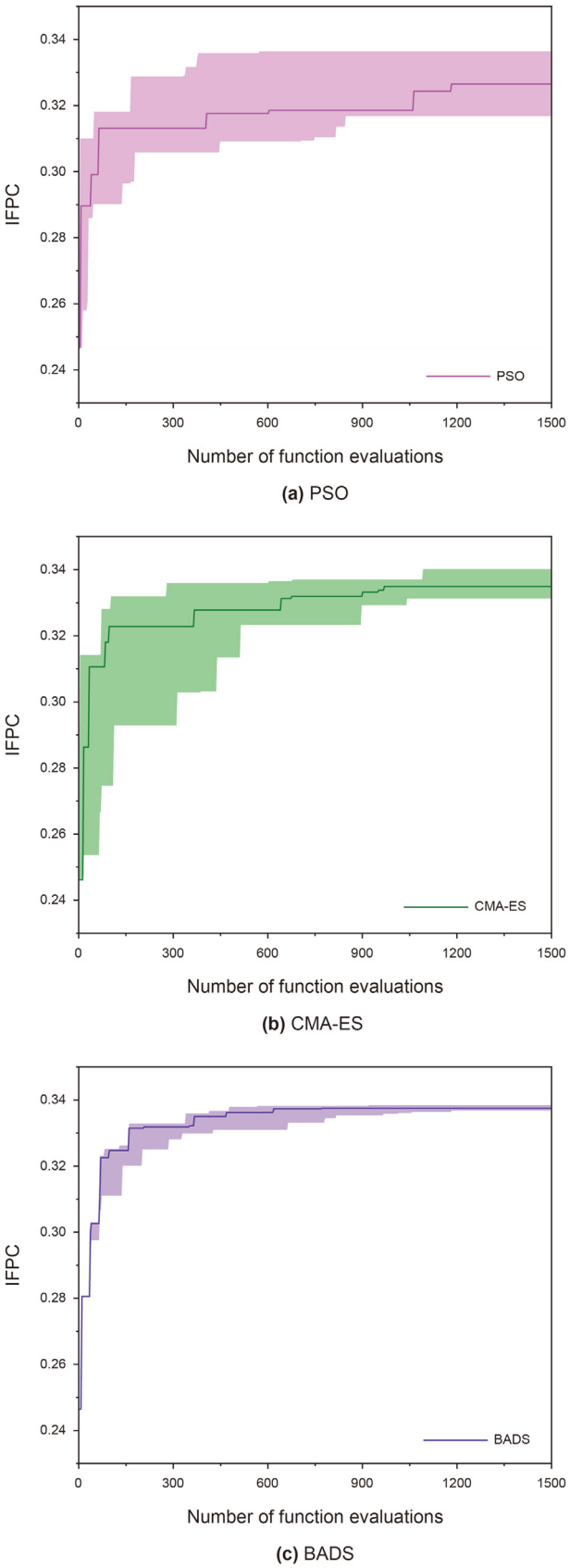

Fig. 11. Convergence progresses of BADS, CMA-ES, and PSO over 10 runs.

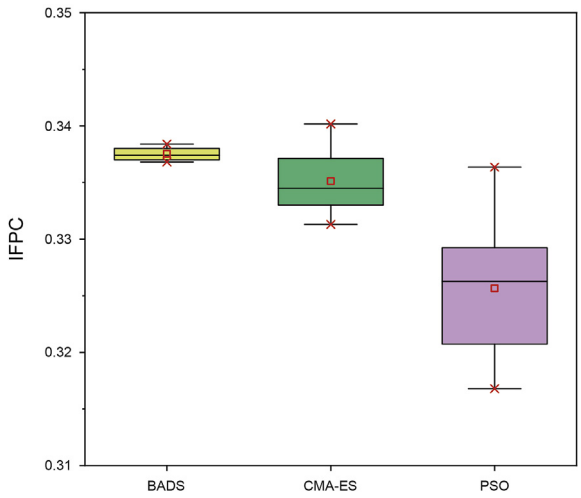

Fig. 12. Boxplot of objective function optimized by PSO, CMA-ES, and BADS in Example II.

Table 5
Results of deterministic algorithms for Example II.

Algorithm	IFPC
GSS	0.3288
MCS	0.3353

4.3. Example III: optimization efficiency of IFPC-based BADS method

This section is still based on the egg model in Section 4.2. In order to illustrate and verify the optimization efficiency and accuracy of the established method, we propose three optimization strategies for comparison.

Strategy A: the problem is optimized by using conventional well production optimization method and only coupling Eclipse with BADS to get maximum cumulative oil production (COP).

Strategy B: optimize this problem only by coupling Eclipse with BADS to get minimum standard deviation of saturation (σ_{S_w}) (Wang, 2016), which is a commonly used as well production optimization method.

Strategy C: optimize this problem by IFPC-based BADS optimization to get the maximum IFPC.

Fig. 13 shows the convergence results of three strategies. We take the average of these 10 times solutions as the optimal well production. The comparison of these three methods' results is listed in Fig. 14.

Strategy A used Eclipse with BADS algorithm to get maximum COP. This method converges after 35 maximum iterations with total CPU time of 88618 s. The calculation process of objective function needs to call the simulator to run until the end of development, which is time-consuming and takes up most of optimization time. The optimal well production is then entered into Eclipse to calculate strategy A's final COP. When the maximum iteration is 31, strategy B reaches convergence condition, and the total CPU time is 81576 s. Strategy C is a new method. We just called a time step in Eclipse and calculated the IFPC. And strategy C only needs 6255 s to obtain the optimal solution from Fig. 14. It can be seen that IFPC-based BADS optimization method is 14.2 times faster than the conventional method (strategy A) and 13 times faster than strategy B. This method can quickly find the best solution, because the IFPC-

Table 6
Results of stochastic algorithms for Example II.

Algorithm	Trials	IFPC			Standard deviation of IFPC
		Maximum	Minimum	Mean	
PSO	10	0.3364	0.3168	0.3263	0.0054
CMA-ES	10	0.3402	0.3313	0.3345	0.0027
BADS	10	0.3384	0.3368	0.3374	0.0005

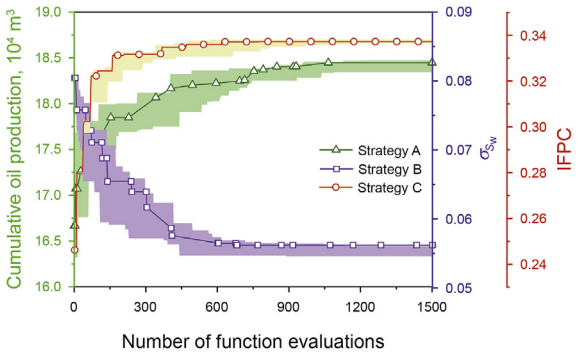

Fig. 13. Convergence of three optimization strategies in example III.

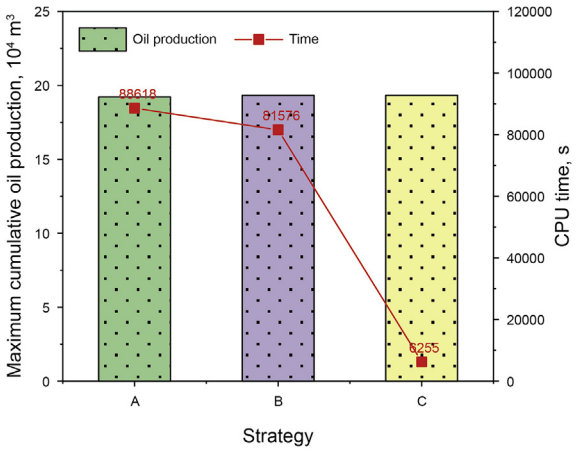

Fig. 14. Comparison of three optimization strategies in example III.

based BADS optimization has the following advantages. The advantage of IFPC-based BADS optimization is that the objective function only needs to call the reservoir numerical simulator to run a time step, instead of calling the simulator to calculate the target value at the end of development. As shown in strategies A and B, the reservoir numerical simulator requires significant time to evaluate the objective function. The egg model is a simple ideal model. If the actual reservoir is used for optimization, the IFPC-based BADS method will have greater advantages in optimization efficiency.

The COP for three strategies versus production time are plotted in Fig. 15(a). And the water cut versus oil recovery between three strategies is also shown in Fig. 15(b). It indicates that strategy A's cumulative oil production is 19.22×10^4 m^3, and strategy B's cumulative oil production is the same as strategy C, both of 19.33×10^4 m^3. The relative error values of cumulative oil production of three strategies are 0.57%, 0.0%, and 0.0%, respectively. Besides, all three strategies increase oil accumulation by more than 15% and improve oil recovery by more than 4.2%. It can be seen that the maximum COP obtained by this method is the same as strategy B and close to strategy A. In addition, the calculation time is 14.2 times faster than the conventional method (strategy A). Therefore, this method can quickly and accurately converge to the optimal solution. If the time-cost is considered, the IFPC-based BADS method, namely strategy C, is a better choice.

The instantaneous streamline distribution optimized by strategy C and oil saturation distribution at the end of production is illustrated in Fig. 16. Besides, Fig. 17 shows the change of fluid volume in individual well before and after optimization. Compared with Fig. 9 before optimization, the saturation distribution after optimization is more balanced. After optimization, the streamline of remaining oil enrichment area is increased and the oil displacement in the enrichment area is accelerated. In addition, the

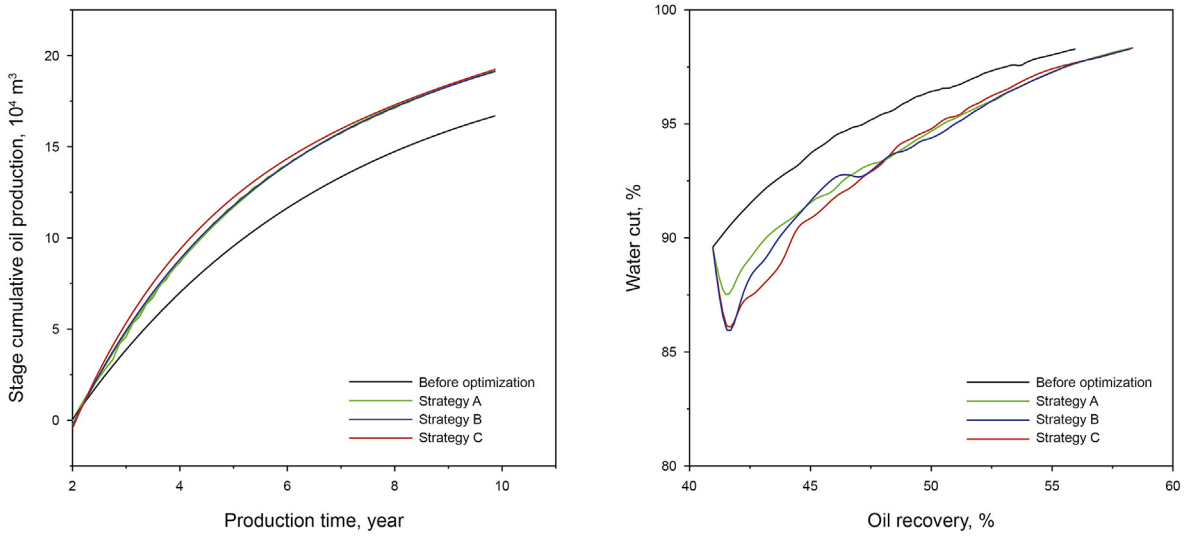

(a) Cumulative oil production versus time

(b) Water cut versus oil recovery

Fig. 15. Cumulative oil production and water cut versus oil recovery for three strategies.

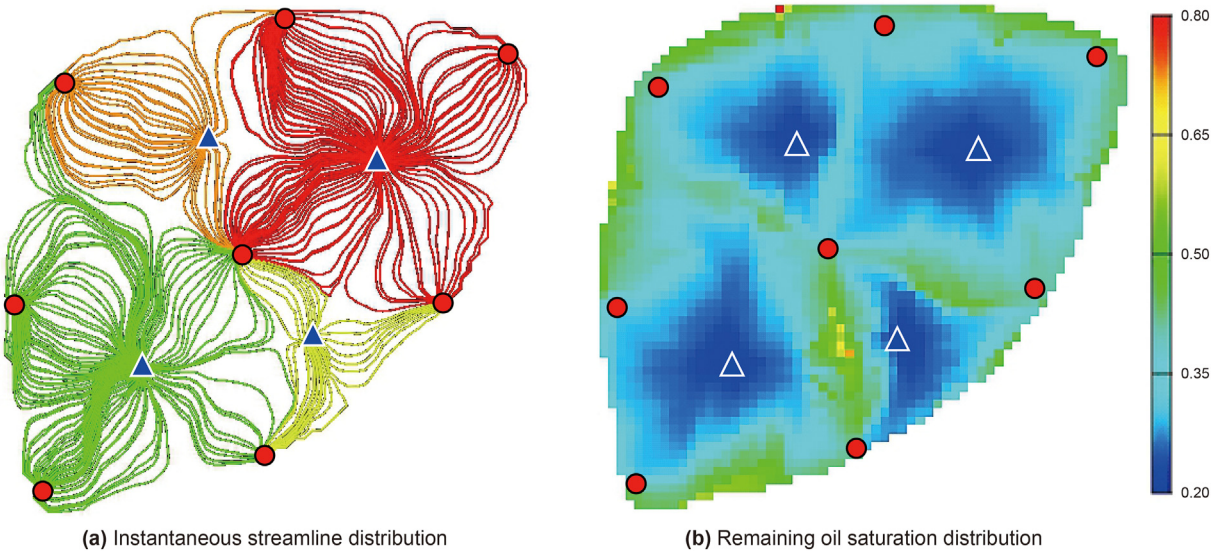

Fig. 16. Streamline and remaining oil saturation distribution optimized by strategy C.

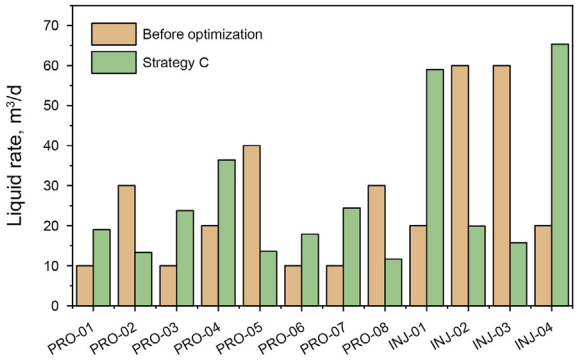

Fig. 17. Injection and production rates for the egg model before and after optimization.

original diversion streamline area becomes the main streamline area, so that the remaining oil that cannot be effectively displaced in the original diversion streamline area can be effectively used. The matching of streamline and well pattern is realized.

5. Conclusions

Well production optimization method based on the streamline features based-objective function and the BADS algorithm is proposed to improve optimization efficiency. The objective function, which represents the water flooding potential, is extracted from streamline features. The index comprehensively considers the influence of movable oil saturation and fluid velocity along streamlines. It only need to call the reservoir numerical simulator to run one time step and calculate the target value, instead of calling the simulator to calculate the target value at the end of development stage, which greatly reduces the running time of the simulator and has significant advantages for large-scale reservoir application. Besides, this new objective function is positively correlated with the cumulative oil production, which verifies its feasibility in well production problems. In addition, the well production optimization model is established and solved by the BADS algorithm based on this objective function. Compared with the GSS, PSO, CMA-ES, and MCS algorithms, the BADS algorithm has advantages in convergence speed, solution stability, and optimization accuracy. Besides, the IFPC-based BADS method can significantly improve the well production optimization efficiency compared with the objective function calculated by traditional method. The method proposed in this paper can help to determine the optimal well production more efficiently for actual oilfield development. Due to the complexity of flow field, the currently established decoding rules for extracting streamline data are appropriate for single-layer reservoirs. For multi-layer reservoirs, it is necessary to determine the longitudinal perforation grid ID between injection-production wells, then use the same method to establish the objective function to optimize the well production.

Acknowledgments

This research is supported partly by the National Science and Technology Major Project of China (Grant No. 2016ZX05025-001-006) and Major Science and Technology Project of CNPC (Grant No. ZD2019-183-007).

References

Acerbi, L., Ma, W.J., 2017. Practical Bayesian optimization for model fitting with Bayesian adaptive direct search. In: 31st Conference on Neural Information Processing Systems (NIPS 2017).

Ahmadpour, M., Siavashi, M., Doranehgard, M.H., 2016. Numerical simulation of two-phase flow in fractured porous media using streamline simulation and IMPES methods and comparing results with a commercial software. J. Cent. S. Univ. 23 (10), 2630–2637. https://doi.org/10.1007/s11771-016-3324-5.

Al-Najem, A.A., Siddiqui, S., Soliman, M., et al., 2012. Streamline simulation technology: evolution and recent trends. SPE Saudi Arabia Section Tech. Symp. Exhib. https://doi.org/10.2118/160894-MS.

AlQahtani, G., Vadapalli, R., Siddiqui, S., et al., 2012. Well optimization strategies in conventional reservoirs. SPE Saudi Arabia Section Tech. Symp. Exhib. https://doi.org/10.2118/160861-MS.

Ambia, F., 2012. A robust optimization tool based on stochastic optimization methods for waterflooding project. SPE Ann. Techn. Conf. Exhib. https://doi.org/10.2118/160907-STU.

Arouri, Y., Sayyafzadeh, M., 2020. Adaptive moment estimation framework for well placement optimization. Comput. Geosci. https://doi.org/10.3997/2214-4609.202035165.

Audet, C., Dennis, J.E., 2006. Mesh adaptive direct search algorithms for constrained optimization. SIAM J. Optim. 17 (1), 188–217. https://doi.org/10.1137/060671267.

Awotunde, A.A., 2014. On the joint optimization of well placement and control. In: SPE Saudi Arabia Section Technical Symposium and Exhibition. https://doi.org/10.2118/172206-MS.

Beckner, B.L., Song, X., 1995. Field development planning using simulated annealing - optimal economic well scheduling and placement. SPE Ann. Tech. Conf. Exhib.

https://doi.org/10.2118/30650-ms.
Bellout, M.C., Ciaurri, D.E., Durlofsky, L.J., et al., 2012. Joint optimization of oil well placement and controls. Comput. Geosci. 16 (4), 1061–1079. https://doi.org/10.1007/s10596-012-9303-5.
Caers, J., 2003. Efficient gradual deformation using a streamline-based proxy method. J. Petrol. Sci. Eng. 39 (1), 57–83. https://doi.org/10.1016/S0920-4105(03)00040-8.
Chen, H.W., Feng, Q.H., Zhang, X.M., et al., 2017. Well placement optimization using an analytical formula-based objective function and cat swarm optimization algorithm. J. Petrol. Sci. Eng. 157, 1067–1083. https://doi.org/10.1016/j.petrol.2017.08.024.
Christie, M.A., Blunt, M.J., 2001. Tenth SPE comparative solution project: a comparison of upscaling techniques. SPE Reservoir Eval. Eng. 4, 308–317. https://doi.org/10.2118/72469-PA.
El-Khatib, N., 1997. Waterflooding performance of communicating stratified reservoirs with log-normal permeability distribution. In: Middle East Oil Show and Conference. https://doi.org/10.2118/59071-PA.
Feng, Q.H., Wang, X., Wang, B., et al., 2013. A dynamic split method to predict development index in heterogeneous waterflooding oil field. SPE Asia Pac. Oil Gas Conf. Exhib. https://doi.org/10.2118/165868-MS.
Feng, Q.H., Wang, X., Wang, D.P., et al., 2014. A streamline simulation method for heterogeneous oil reservoirs considering permeability tensor. J. China Univ. Petrol. (Ed. Nat. Sci.) 38 (1), 75–80. https://doi.org/10.3969/j.issn.1673-5005.2014.01.011 (in Chinese).
Fonseca, R.M.M., Leeuwenburgh, O., Rossa, E.D., et al., 2015. Ensemble-based multi-objective optimization of on-off control devices under geological uncertainty. SPE Reservoir Eval. Eng. 18, 554–563. https://doi.org/10.2118/173268-PA, 04.
GeoQuest, S., 2016. Eclipse Reference Manual. Schlumberger, Houston, TX.
Ghori, S.G., Syed, Z.J., Vohra, L.R., et al., 2006. Improving injector efficiency using streamline simulation: a case study of waterflooding in Saudi Arabia. In: SPE/DOE Symposium on Improved Oil Recovery. https://doi.org/10.2118/93031-MS.
Gladkov, A., Fondakov, D., Gareev, R., et al., 2013. Streamlines for the target injection calculation in complex field conditions. In: SPE Arctic and Extreme Environments Technical Conference and Exhibition. https://doi.org/10.2118/166874-MS.
Goda, H.M., Behrenbruch, P., 2004. Using a modified Brooks-Corey model to study oil-water relative permeability for diverse pore structures. In: SPE Asia Pacific Oil and Gas Conference and Exhibition. https://doi.org/10.2118/88538-MS.
Gramacy, R., Le Digabel, S., 2015. The mesh adaptive direct search algorithm with treed Gaussian process surrogates. Pac. J. Optim. 11 (3), 419–447. WOS: 000360418500001.
Hansen, N., Kern, S., 2004. Evaluating the CMA evolution strategy on multimodal test functions. In: International Conference on Parallel Problem Solving from Nature. https://doi.org/10.1007/978-3-540-30217-9_29.
He, J., Xie, J., Wen, X.H., et al., 2016. An alternative proxy for history matching using proxy-for-data approach and reduced order modeling. J. Petrol. Sci. Eng. 146 (1), 392–399. https://doi.org/10.1016/j.petrol.2016.05.026.
Isebor, O.J., Durlofsky, L.J., Ciaurri, D.E., et al., 2014. A derivative-free methodology with local and global search for the constrained joint optimization of well locations and controls. Comput. Geosci. 18 (3), 463–482. https://doi.org/10.1007/s10596-013-9383-x.
Jansen, J.D., Fonseca, R.M., Kahorbaei, S., et al., 2015. The egg model - a geological ensemble for reservoir simulation. Geosci. Data J. 1 (2), 192–195. https://doi.org/10.1002/gdj3.21.
Jesmani, M., Bellout, M.C., Hanea, R., et al., 2016. Well placement optimization subject to realistic field development constraints. Comput. Geosci. 20 (6), 1185–1209. https://doi.org/10.1007/s10596-016-9584-1.
Jimenez, E., Sabir, K., Datta-Gupta, A., et al., 2005. Spatial error and convergence in streamline simulation. SPE Reservoir Simul. Symp. 10, 221–232. https://doi.org/10.2118/92873-MS.
Jones, D.R., Schonlau, M., Welch, W.J., 1998. Efficient global optimization of expensive black-box functions. J. Global Optim. 13 (4), 455–492. https://doi.org/10.1023/A:1008306431147.
Knudsen, B.R., Foss, B., 2015. Designing shale-well proxy models for field development and production optimization problems. J. Nat. Gas Sci. Eng. 27, 504–514. https://doi.org/10.1016/j.jngse.2015.08.005.
Lambot, S., Javaux, M., Hupet, F., 2002. A global multilevel coordinate search procedure for estimating the unsaturated soil hydraulic properties. Water Resour. Res. 38 (11), 1–15. https://doi.org/10.1029/2001WR001224.
Li, L., Jafarpour, B., Mohammad, M.R., 2013. A simultaneous perturbation stochastic approximation algorithm for coupled well placement and control optimization under geologic uncertainty. Comput. Geosci. 17 (1), 167–188. https://doi.org/10.1007/s10596-012-9323-1.
Li, S.S., Feng, Q.H., Zhang, X.M., et al., 2022. Flow field characterization and evaluation method based on unsupervised machine learning. J. Petrol. Sci. Eng. 215, 110599. https://doi.org/10.1016/j.petrol.2022.110599.
Liu, Z., 2018. Study on Optimization of Injection and Production Adjustment Based on Differential Evolution. M.S. Thesis. Qingdao. China University of Petroleum.
Lv, Q., 2009. The Research of Numerical Simulation of Reservoir by Streamline. M.S. Thesis. China University of Petroleum, Qingdao.
Mahjour, S.K., Silva, L.O., Meira, L.A., et al., 2022. Evaluation of unsupervised machine learning frameworks to select representative geological realizations for uncertainty quantification. J. Petrol. Sci. Eng. 209, 109822. https://doi.org/10.1016/j.petrol.2021.109822.
MATLAB, R., 2019. Version 9.7.0.1190202. The MathWorks Inc, Natick. R2019b.
Mollaei, A., Delshad, M., 2019. Introducing a novel model and tool for design and performance forecasting of waterflood projects. Fuel 237, 298–307. https://doi.org/10.1016/j.fuel.2018.09.125.
Nasir, Y., Yu, W., Sepehrnoori, K., 2020. Hybrid derivative-free technique and effective machine learning surrogate for nonlinear constrained well placement and production optimization. J. Petrol. Sci. Eng. 186, 106726. https://doi.org/10.1016/j.petrol.2019.106726.
Nwankwor, E., Nagar, A.K., Reid, D.C., 2013. Hybrid differential evolution and particle swarm optimization for optimal well placement. Comput. Geosci. 17 (2), 249–268. https://doi.org/10.1007/s10596-012-9328-9.
Oliveira, D.F.F., Reynolds, A., 2014. An adaptive hierarchical multiscale algorithm for estimation of optimal well controls. SPE J. 19, 909–930. https://doi.org/10.2118/163645-PA.
Onwunalu, J.E., Litvak, M.L., Durlofsky, L.J., et al., 2008. Application of statistical proxies to speed up field development optimization procedures. In: Abu Dhabi International Petroleum Exhibition and Conference. https://doi.org/10.2118/117323-MS.
Osako, I., Kumar, M., Hoang, V.T., et al., 2009. Evaluation of streamline simulation application to heavy oil waterflood. In: Latin American and Caribbean Petroleum Engineering Conference. https://doi.org/10.2118/122922-MS.
Perez, R., Behdinan, K., 2007. Particle swarm approach for structural design optimization. Comput. Struct. 85 (19), 1579–1588. https://doi.org/10.1016/j.compstruc.2006.10.013.
Pollock, D.W., 1988. Semianalytical computation of path lines for finite-difference models. Groundwater 26 (6), 743–750. https://doi.org/10.1111/j.1745-6584.1988.tb00425.x.
Pouladi, B., Karkevandi-Talkhooncheh, A., Sharifi, M., et al., 2020. Enhancement of SPSA algorithm performance using reservoir quality maps: application to coupled well placement and control optimization problems. J. Petrol. Sci. Eng. 189, 106984. https://doi.org/10.1016/j.petrol.2020.106984.
Salehian, M., Sefat, M.H., Muradov, K., 2021. Robust integrated optimization of well placement and control under field production constraints. J. Petrol. Sci. Eng. 205, 108926. https://doi.org/10.1016/j.petrol.2021.108926.
Sampaio, M.A., Barreto, C.E., Schiozer, D.J., 2015. Assisted optimization method for comparison between conventional and intelligent producers considering uncertainties. J. Petrol. Sci. Eng. 133, 268–279. https://doi.org/10.1016/j.petrol.2015.06.023.
Sarma, P., Aziz, K., Durlofsky, L.J., 2005. Implementation of adjoint solution for optimal control of smart wells. In: SPE Reservoir Simulation Symposium. https://doi.org/10.2118/92864-MS.
Schlumberger, C., 2015. Frontsim Technical Description.
Semnani, A., Yu, Y., Ostadhassan, M., 2022. Joint optimization of constrained well placement and control parameters with a quantum-inspired cell-based quality gate function. J. Petrol. Sci. Eng. 209, 109854. https://doi.org/10.1016/j.petrol.2021.109854.
Siavashi, M., Pourafshary, P., Raisee, M., 2012. Application of space–time conservation element and solution element method in streamline simulation. J. Petrol. Sci. Eng. 96–97, 58–67. https://doi.org/10.1016/j.petrol.2012.08.005.
Siavashi, M., Tehrani, M.R., Nakhaee, A., 2016. Efficient particle swarm optimization of well placement to enhance oil recovery using a novel streamline-based objective function. J. Energy Resour. Technol. 138 (5). https://doi.org/10.1115/1.4032547.
Tavallali, M.S., Karimi, I.A., Teo, K.M., et al., 2013. Optimal producer well placement and production planning in an oil reservoir. Comput. Chem. Eng. 55, 109–125. https://doi.org/10.1016/j.compchemeng.2013.04.002.
Thiele, M.R., Batycky, R.P., 2003. Water injection optimization using a streamline-based workflow. In: SPE Annual Technical Conference and Exhibition. https://doi.org/10.2118/84080-MS.
Tsai, J.T., 2015. Improved differential evolution algorithm for nonlinear programming and engineering design problems. Neurocomputing 148 (1), 628–640. https://doi.org/10.1016/j.neucom.2014.07.001.
Wang, L., Yao, Y., Zhang, T., et al., 2022. A novel self-adaptive multi-fidelity surrogate-assisted multi-objective evolutionary algorithm for simulation-based production optimization. J. Petrol. Sci. Eng. 211, 110111. https://doi.org/10.1016/j.petrol.2022.110111.
Wang, X., Haynes, R.D., Feng, Q.H., 2016. A multilevel coordinate search algorithm for well placement, control and joint optimization. Comput. Chem. Eng. 95 (1), 75–96. https://doi.org/10.1016/j.compchemeng.2016.09.006.
Wang, X., Haynes, R.D., He, Y., et al., 2019. Well control optimization using derivative-free algorithms and a multiscale approach. Comput. Chem. Eng. 123 (1), 12–33. https://doi.org/10.1016/j.compchemeng.2018.12.004.
Wang, X., Feng, Q.H., Haynes, R.D., 2015. Optimization of well placement and production for large-scale mature oil fields. J. Eng. Sci. Technol. Rev. 8 (5), 134–140.
Wang, L., Zhang, L., Lai, F., et al., 2019. Multi-objective optimization design of reservoir injection-production parameters based on substitution model. Sci. Technol. Eng. 19 (26), 178–185.
Wang, X., 2016. Well Placement and Production Optimization for Water Flooding Oilfields. Ph.D. Dissertation. Qingdao: China University of Petroleum.
Wu, J., Li, Z., Sun, Y., et al., 2020. Neural network-based prediction of remaining oil distribution and optimization of injection-production parameters. Petrol. Geol. Recov. Effic. 27 (4), 85–93. https://doi.org/10.13673/j.cnki.cn37-1359/te.2020.04.010 (in Chinese).
Yan, X., Li, Y., Yao, J., et al., 2013. Reservoir production optimization method based on modified simplex gradient algorithm. Petrol. Geol. Recov. Effic. 20 (3), 65–67 (in Chinese).

Yeten, B., 2003. Optimum Deployment of Nonconventional Wells. Ph.D Dissertation. Stanford University, Stanford.

Zhang, K., Zhao, X.G., Zhang, L., et al., 2020. Current status and prospect for the research and application of big data and intelligent optimization methods in oilfield development. J. China Univ. Petrol. (Ed. Nat. Sci.) 44 (4), 28–38. https://doi.org/10.3969/j.issn.1673-5005.2020.04.004 (in Chinese).

Zhang, X., 2018. Production Optimization Study Based on Cooperative Multi-Objective Artificial Bee Colony Algorithm. M.S. Thesis. China University of Petroleum, Qingdao.

Zhou, Z., Ong, Y.S., Nair, P.B., et al., 2007. Combining global and local surrogate models to accelerate evolutionary optimization. IEEE Trans. Syst. Man Cybern. C 37 (1), 66–76. https://doi.org/10.1109/TSMCC.2005.855506.